



COMPARISON OF SGS MODELS IN LARGE-EDDY SIMULATION FOR TRANSITION TO TURBULENCE IN TAYLOR-GREEN FLOW

Ilyas YILMAZ¹, Lars DAVIDSON²

¹ Corresponding Author. Department of Mechanical Engineering, Faculty of Engineering, Istanbul Aydin University. Florya, 34295, Istanbul, Turkey. Tel.: +90 212 444 1 428, Fax: +90 212 425 57 59, E-mail: ilyasyilmaz@aydin.edu.tr ¹

² Division of Fluid Dynamics, Department of Applied Mechanics, Chalmers University of Technology. SE-412 96 Gothenburg, Sweden. Tel. +46 31 772 14 04, Fax. +46 31 18 09 76, E-mail: lada@chalmers.se

ABSTRACT

A study was done to observe and to analyze the behavior of various Sub-Grid Scale (SGS) models in Large-Eddy Simulation (LES) for the flow where laminar, transitional and turbulent regimes are found during the evolution. Taylor-Green Vortex (TGV) flow which shows the fundamental mechanisms of vortex stretching and breakdown, transition to turbulence and turbulent decay was selected as a challenging test case for this study. It is initially laminar at early times. However, the effects of viscous interactions result in vortex breakdown and disordering of initially well-organized structures and the flow undergoes transition to turbulence and decays in time. From this point of view, it may serve as a prototype for industrial flows where the flow regimes can change rapidly. The tested SGS models are the Smagorinsky, the dynamic Smagorinsky, the Vreman model, the WALE model and the one-equation model. All the models tested capture the overall physics of TGV flow. However, differences are observed mainly during transition. It is under- or over-predicted slightly, depending on the grid resolution. The SGS models capable of scaling their inherent dissipations produced better results when comparable with the reference DNS solutions.

Keywords: Large-Eddy Simulation, Sub-Grid Scale modeling, Taylor-Green Vortex flow, Transition to turbulence

NOMENCLATURE

<i>DNS</i>	Direct Numerical Simulation
<i>LES</i>	Large-Eddy Simulation
<i>RANS</i>	Reynolds-Averaged Navier-Stokes
<i>SGS</i>	Sub-Grid Scale
<i>TGV</i>	Taylor-Green Vortex
<i>WALE</i>	Wall-Adapting Local Eddy-Viscosity

K	Mean resolved kinetic energy
L	Domain length
Q	Vortex detection criterion based on the 2 nd invariant of the velocity gradient tensor
$S(n)$	High-order velocity-derivative moments, skewness (n=3) and flatness (n=4)
U	Characteristic velocity
$-\frac{dK}{dt}$	Dissipation of resolved kinetic energy
$C_s, C_W, C_k, C_\epsilon$	Constants in SGS models
$P_{k_{sgs}}$	Production term
Re	Reynolds number
Re_λ	Taylor micro-scale Reynolds number
S_{ij}	Strain-rate tensor tensor
Δ	Grid size
δ_{ij}	Kronecker delta
λ	Taylor micro-scale
\mathbf{u}	velocity vector
∇	Nabla operator
ν	Kinematic viscosity
ν_{sgs}	Sub-grid scale kinematic viscosity
ω	Vorticity
ω^2	Enstrophy
ρ, ρ_0	Density, Initial density
τ	Non-dimensional time
τ_{ij}	Sub-grid scale stress tensor
g_{ij}	Velocity gradient tensor
k	Wave number
k_{sgs}	Sub-grid scale kinetic energy
p, p_0, p_∞	Pressure, initial pressure, ref. pressure
t	Time
u_0, v_0, w_0	Initial velocity field
u_i	Velocity component
x_i	Space component

Subscripts and Superscripts

$\langle \rangle$	Space averaged
$\bar{}$	Grid filtered
$\tilde{}$	Test filtered
rms	Root mean square

¹Present address: Division of Fluid Dynamics, Department of Applied Mechanics, Chalmers University of Technology, 412 96, Gothenburg, Sweden, E-mail:ilyasy@chalmers.se

1. INTRODUCTION

Most of industrial and engineering flows are inherently turbulent. They may also be transitional, i.e., subject to rapid changes in their flow regimes in both time and space due to structural necessities, instabilities in their origins, surface porosity, heat effects, etc. Their transitional/turbulent behaviors must be predicted accurately to prevent high costs and to make the flows feasible as well. Numerically, the most direct way on ensuring this is Direct Numerical Simulation (DNS). In DNS, all the scales of turbulent are resolved properly. However, due to its excessive grid resolution and time-step requirements, it is only available for relatively low Reynolds number flows in simple geometries. The Reynolds-Averaged Navier-Stokes (RANS) approach, which models all the scales, has been used for many years with a reduced accuracy and limited capability. Nowadays, RANS is not accomplishing current demands of engineering. As a result, Large-Eddy Simulation (LES), where most of the scales are resolved by grid and the contributions coming from the Sub-Grid Scales (SGS) are modeled, is becoming a natural choice.

LES is attractive method since it has a balance among accuracy, capability, numerical cost and industrial/engineering demands. The major drawback of LES is lacking of a universal SGS model which is equally applicable to all kinds of flows including curvature, separation-reattachment, buoyancy, heat transfer, etc. Because of this reason, LES research mainly focuses on developing efficient SGS models and its applications. Since choosing appropriate models can not directly be known a priori, analyzing the behavior of models and comparing them are always useful for many purposes, as it has been done by many researchers for various flows.

In this study, we perform LES of Taylor-Green Vortex (TGV) flow with five different SGS models. TGV is the simplest fundamental flow that represents vortex stretching and energy cascade processes that lead to turbulence[1]. Initially, it is well-organized and laminar. At later times, the viscous diffusion plays an important role in dynamics and distorted structures are formed. The decay rate of the kinetic energy reaches its peak after a couple of *eddy-turnover time*, around ≈ 9 . Then the flow structures die out due to the viscosity, following approximately the power-law spectrum. This transitional behavior is entirely determined by the viscosity. For Reynolds number, $Re \geq 1000$, this picture becomes very clear[2]. Numerically, the kinetic energy should be preserved during the inviscid simulations, due to the lack of the viscous effects.

TGV basically represents the mechanism of transition to turbulence and its decay. From this point of view, it can be regarded as a canonical example to some industrial/engineering flows and serve as an appropriate test case for especially turbulence modeling approaches.

The outline of the paper is as follows. Section 2 briefly describes the governing equation in LES, SGS models used in this study and the solver as well. Section 3 provides information about the numerical setup of TGV flow. Section 4 presents the results with detailed analyses and discussions.

2. SIMULATION METHODOLOGY

The central differencing finite-volume method was used to discretize the governing equations on a collocated grid. Second-order Crank-Nicolson scheme was employed for time advancement[3]. The numerical procedure is based on an implicit fractional step technique combined with an efficient multi-grid pressure Poisson solver [4].

The grid-filtered incompressible Navier-Stokes equations in LES read

$$\begin{aligned} \frac{\partial \bar{u}_i}{\partial x_i} &= 0 \\ \frac{\partial \bar{u}_i}{\partial t} + \frac{\partial}{\partial x_j}(\bar{u}_i \bar{u}_j) &= -\frac{1}{\rho} \frac{\partial \bar{p}}{\partial x_i} + \nu \frac{\partial^2 \bar{u}_i}{\partial x_j \partial x_j} - \frac{\partial \tau_{ij}}{\partial x_j} \end{aligned} \quad (1)$$

Here, τ_{ij} are the SGS stresses given as $\overline{u_i u_j} - \bar{u}_i \bar{u}_j$.

Most SGS models are eddy-viscosity models of the form ,

$$\tau_{ij} - \frac{\delta_{ij}}{3} \tau_{kk} = -2\nu_{sgs} \bar{S}_{ij} \quad (2)$$

which relates the SGS stresses to the large-scale strain rate tensor, \bar{S}_{ij} ,

$$\bar{S}_{ij} = \frac{1}{2} \left(\frac{\partial \bar{u}_i}{\partial x_j} + \frac{\partial \bar{u}_j}{\partial x_i} \right) \quad (3)$$

The SGS models used in this study are the Smagorinsky, the dynamic Smagorinsky, the Wale model, the Vreman model and the one-equation model of Yoshizawa. While the first four models compute ν_{sgs} only using algebraic relations, the Yoshizawa one-equation model solves an additional equation for SGS kinetic energy, k_{sgs} .

For the Smagorinsky model[5], ν_{sgs} is obtained via

$$\nu_{sgs} = (C_s \Delta)^2 |\bar{S}| \quad (4)$$

where $|\bar{S}| = \sqrt{2\bar{S}_{ij}\bar{S}_{ij}}$. The Smagorinsky constant, C_s , is set to 0.1 and Δ is equal to grid size.

The dynamic Smagorinsky model tested here is the one proposed in [6]. It uses the same analogy with the Smagorinsky model. However, C_s in Eq.4 is not constant anymore. Instead, it is computed dynamically using a test filter as

$$C_s = \frac{1}{2} = \frac{D_{ij} P_{ij}}{P_{ij} P_{ij}} \quad (5)$$

Here,

$$\begin{aligned} D_{ij} &= T_{ij} - \tilde{\tau}_{ij} \\ T_{ij} - \frac{\delta_{ij}}{3} T_{kk} &= -2C_s^2 \tilde{\Delta}^2 |\tilde{S}| \tilde{S}_{ij} \\ P_{ij} &= \Delta^2 |\tilde{S}| \tilde{S}_{ij} - \tilde{\Delta}^2 |\tilde{S}| \tilde{S}_{ij} \end{aligned} \quad (6)$$

where $(\tilde{\cdot})$ denotes the test filter usually taken as twice the grid filter and T_{ij} is the SGS stresses on the test filter. This model allows *backscattering*, i.e., negative C_s from the small scales to the resolved flow.

The Wall-Adapting Local Eddy-Viscosity (WALE) model[7] employs the traceless symmetric part of the square of the velocity gradient tensor which is

$$S_{ij}^d = \frac{1}{2} (\bar{g}_{ij}^2 + \bar{g}_{ji}^2) - \frac{1}{3} \delta_{ij} \bar{g}_{kk}^2 \quad (7)$$

and calculates ν_{sgs} using

$$\nu_{sgs} = (C_W \Delta)^2 \frac{(S_{ij}^d S_{ij}^d)^{3/2}}{(\bar{S}_{ij} \bar{S}_{ij})^{5/2} + (S_{ij}^d S_{ij}^d)^{5/4}} \quad (8)$$

with $C_W = 0.33$.

The Vreman model[8] is also an eddy-viscosity model that has the following algebraic relation

$$\nu_{sgs} = 2.5 C_s^2 \sqrt{\frac{B_\beta}{\alpha_{ij} \alpha_{ij}}} \quad (9)$$

with

$$\begin{aligned} \alpha_{ij} &= \frac{\partial \bar{u}_j}{\partial x_i} \\ \beta_{ij} &= \Delta_m^2 \alpha_{mi} \alpha_{mj} \\ B_\beta &= \beta_{11} \beta_{12} - \beta_{12}^2 + \beta_{11} \beta_{33} - \beta_{13}^2 + \beta_{22} \beta_{33} - \beta_{23}^2 \end{aligned} \quad (10)$$

The last model introduced here is the one-equation model by Yoshizawa[9]. The SGS kinetic energy equation solved by the model reads

$$\begin{aligned} \frac{\partial k_{sgs}}{\partial t} + \frac{\partial}{\partial x_j} (\bar{u}_j k_{sgs}) \\ = \frac{\partial}{\partial x_j} \left[(\nu + \nu_{sgs}) \frac{\partial k_{sgs}}{\partial x_j} \right] + P_{k_{sgs}} - C_\epsilon \frac{k_{sgs}^{3/2}}{\Delta} \end{aligned} \quad (11)$$

with $P_{k_{sgs}} = 2\nu_{sgs} \bar{S}_{ij} \bar{S}_{ij}$, $\nu_{sgs} = C_k \Delta k_{sgs}^{1/2}$, $C_k = 0.07$ and $C_\epsilon = 1.05$.

Due to the formulations, the SGS models presented here, except the constant Smagorinsky model, theoretically have capability to detect flow regions including transitional, laminar, shear, wall and to scale or vanish their SGS dissipations properly.

3. FLOW SETUP

The initial velocity field is given by

$$\begin{aligned} u_0 &= U \sin(kx) \cos(ky) \cos(kz) \\ v_0 &= -U \cos(kx) \sin(ky) \cos(kz) \\ w_0 &= 0 \end{aligned} \quad (12)$$

and the initial pressure field provided by the solution of the Poisson equation is

$$p_0 = p_\infty + (\rho_0 U^2 / 16) (2 + \cos(2kz)) (\cos(2kx) \cos(2ky)) \quad (13)$$

where k is the wave number, $\frac{2\pi}{L}$. L is the domain length 2π .

Boundaries are triply-periodic. Since the characteristic velocity is bounded by the unity and the characteristic length is set to 1, the Reynolds number is defined as the inverse of the kinematic viscosity, $1/\nu$ and set to 1600. This also leads to an *eddy-turnover time* of order unity. The Taylor micro-scale Re number (Re_λ) can be defined as $\sqrt{2Re}$, giving an initial value of 55. Simulations were performed on uniform 64^3 and 128^3 grids and followed up to 15 non-dimensional time-units with a time-step of 2.5×10^{-2} .

4. RESULTS AND DISCUSSION

Fig.1 shows how the initially well-organized structures lose their symmetries in time due to the energy cascade and the vortex stretching and start to break into smaller ones.

Fig.2 compares various flow diagnostics such as evolution of the mean resolved kinetic energy (K), skewness, flatness and Taylor micro-scale λ computed by each model. K , which is computed as $K = \frac{1}{2} \langle \bar{u}_i \rangle^2$, decreases due to increase in dynamic, viscous interactions. Skewness ($n = 3$) and flatness ($n = 4$) are the high-order velocity-derivative moments (structure functions) given by

$$S(n) = \frac{1}{3} \sum S_i(n) \quad (14)$$

where

$$S_i(n) = (-1)^n \frac{\langle (\frac{\partial \bar{u}_i}{\partial x_i})^n \rangle}{\langle (\frac{\partial \bar{u}_i}{\partial x_i})^2 \rangle^{n/2}} \quad (\text{no summation on } i) \quad (15)$$

The skewness characterizes the rate at which enstrophy increases by vortex stretching. Whereas, the flatness is a measure of the intermittency of the vorticity field driven by vortex stretching and folding. Their average values given in the literature change from 0.2 to 0.7 for skewness, and from 3 to 40 for flatness [10]. All the models produce similar results which are in the given range and show the same behavior. The largest discrepancies between model results and the reference solution are observed in skewness, both around $t/\tau \approx 4$ and around transition time. The same discrepancy was also observed by Hahn[11].

The Taylor micro-scale averaged over the three homogeneous spatial directions is given as,

$$\lambda = \frac{1}{3} \sum \lambda_i \quad (16)$$

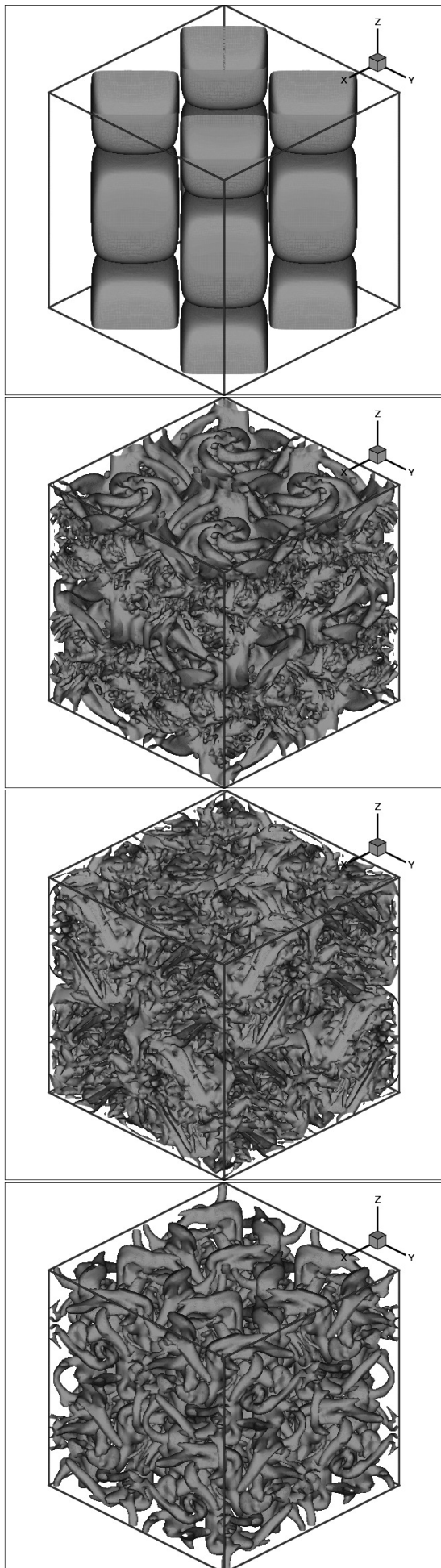
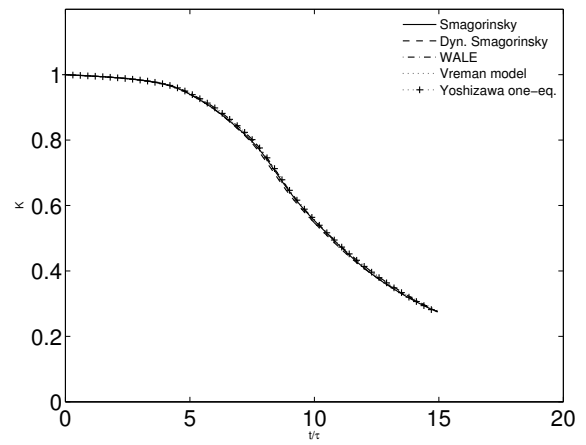
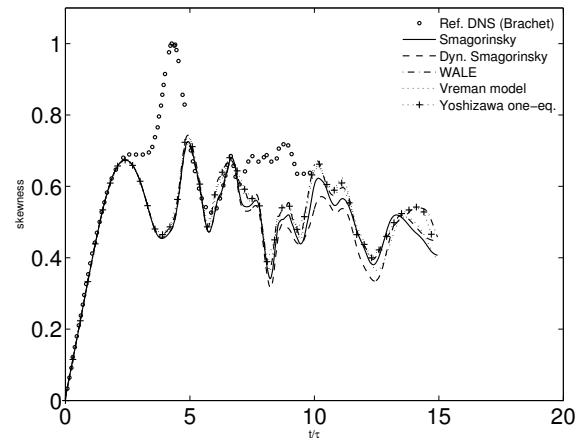


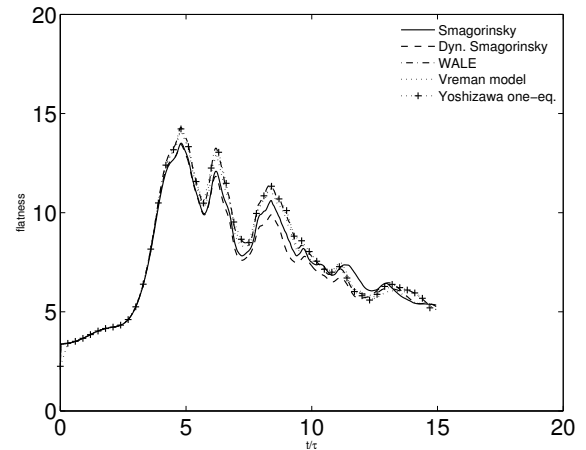
Figure 1. $Q = -\frac{1}{2} \frac{\partial u_i}{\partial x_j} \frac{\partial u_j}{\partial x_i}$ iso-surfaces at $\tau = 0, 10, 20, 50$ from top to bottom respectively. ($Q = 0.019$)



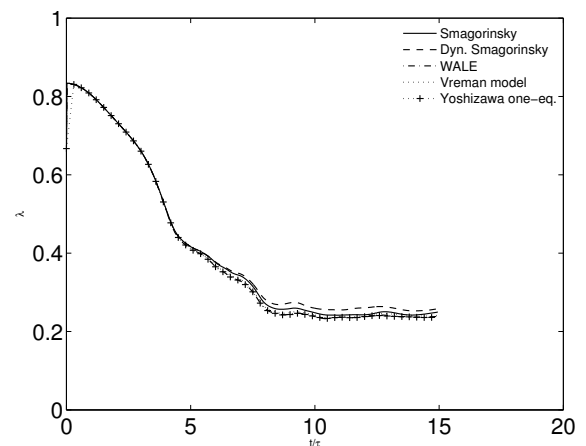
(a) Mean resolved kinetic energy



(b) Skewness



(c) Flatness



(d) λ

Figure 2. Evolution of various flow diagnostics in time on fine grid

where

$$\lambda_i = \sqrt{\frac{\langle (u_i)_{rms}^2 \rangle}{\langle (\frac{\partial \bar{u}_i}{\partial x_i})^2 \rangle}} \quad (\text{no summation on } i) \quad (17)$$

The Taylor micro-scale is a length scale which was first introduced by Taylor[12]. It does not have an exact physical meaning [13]. However, it is often used to define a Reynolds number that characterizes grid turbulence [14]. It is an intermediate length scale between integral and Kolmogorov's length scales. It is roughly assumed that, below the Taylor micro-scale, fluid viscosity significantly affects the dynamics of turbulent eddies in the flow, the turbulent motions are subject to strong viscous forces, and kinetic energy is dissipated into heat [15].

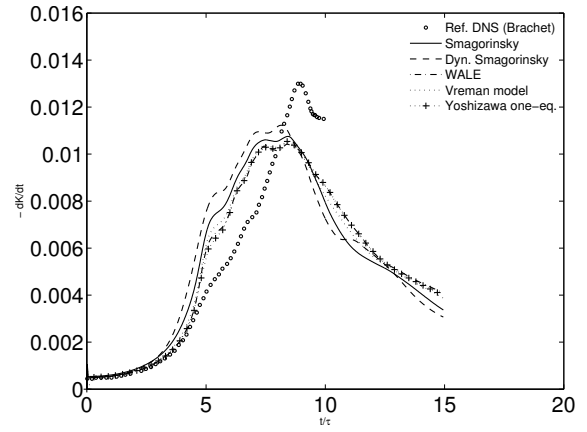
In Fig.3, the dissipation of mean resolved kinetic energies, $-dK/dt$, are plotted for different resolutions. Zoomed view of the transition peaks are also provided. It seems that all the SGS models included here are having difficulties in handling transition to turbulence in time. Regardless of the grid resolution, the transition time is predicted slightly earlier ($t/\tau_{sim} \approx 8.2$) by the models than the reference DNS solution ($t/\tau_{DNS} \approx 9$). This behavior corresponds to over dissipative nature of the SGS models for transition. Additionally, while the value of the transition peak is higher than the reference on the fine grid, on the coarse grid, it is vice versa. It points out an increasing dissipation of mean resolved kinetic energy with an increasing resolution. All the models also have different peak structures. The Smagorinsky and the dynamic Smagorinsky models show the most noticeable differences among the models.

The mean enstrophy is given as the square of vorticity(ω),

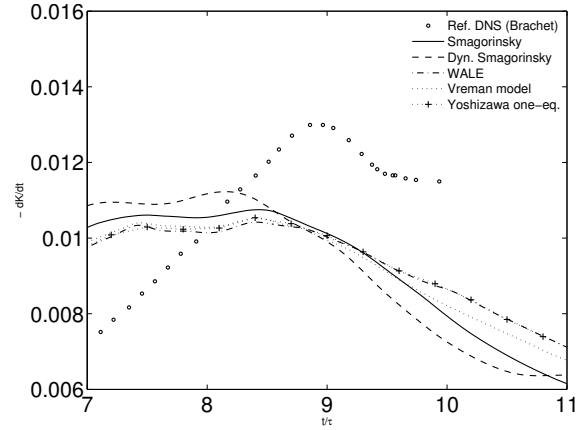
$$\langle \bar{\omega}^2 \rangle = \langle |\nabla \times \bar{\mathbf{u}}|^2 \rangle \quad (18)$$

Enstrophy is the resolving power of a numerical scheme that is a measure of its ability to represent the flow physics accurately on a finite number of grid cells [16]. As seen in Fig. 4, it follows a path similar to the mean kinetic energy dissipation. Its value predicted by the models increases with increasing grid resolution which points out high resolution requirement of models. The Yoshizawa one-equation model, the Vreman model and the WALE model show noticeably better performance, as it should be because of their advanced differential operators in finding C_s and computing v_{sgs} .

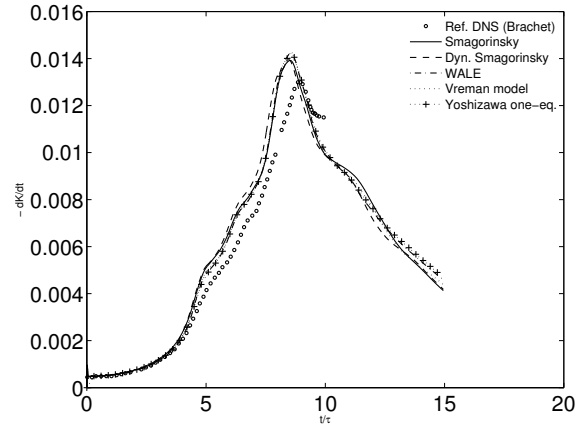
The SGS viscosities plotted in Fig. 5a and 5b are one of the most important quantities to make some assessment when doing LES. First of all, no backscattering is predicted by the models. The Smagorinsky and the Dynamic Smagorinsky models behave completely different than the others. Their computed v_{sgs} values are strongly depend on the grid resolution. The Yoshizawa one-equation model have a very smooth path in time, while evolution of the others are relatively fluctuating in time.



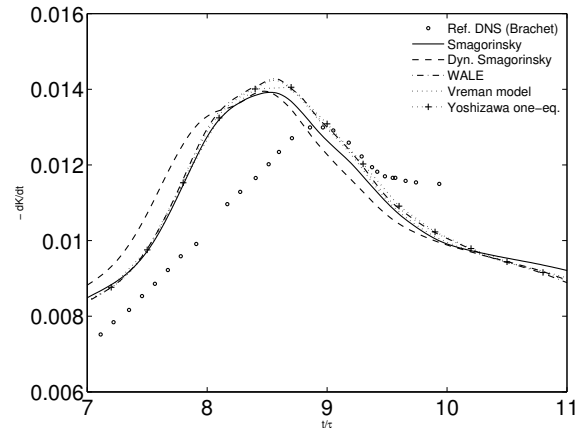
(a) Coarse grid (64^3)



(b) Zoom to transition peak (64^3)

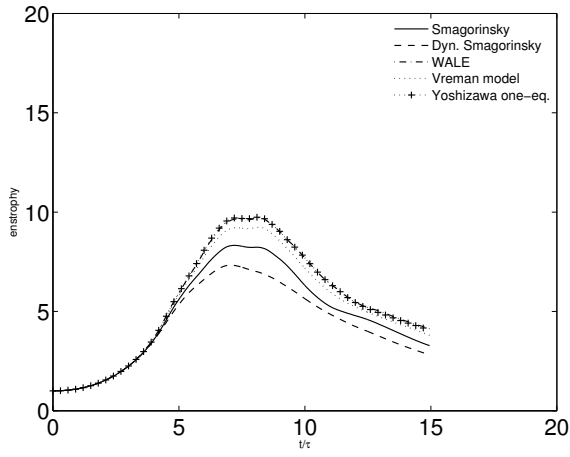


(c) Fine grid (128^3)

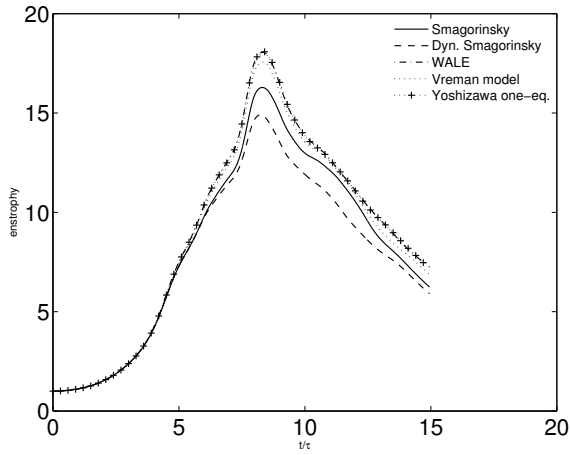


(d) Zoom to transition peak (128^3)

Figure 3. Dissipation of mean resolv. kin. energy



(a) Coarse grid (64^3)

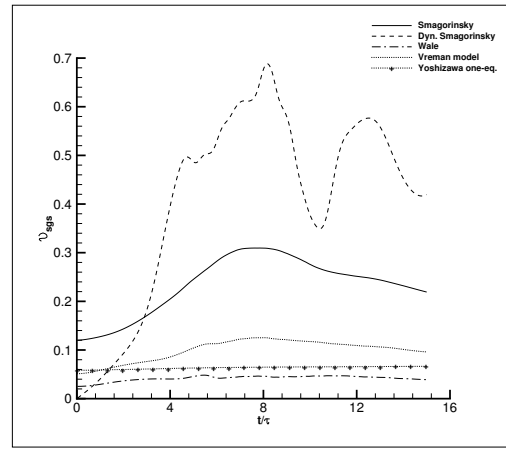


(b) Fine grid (128^3)

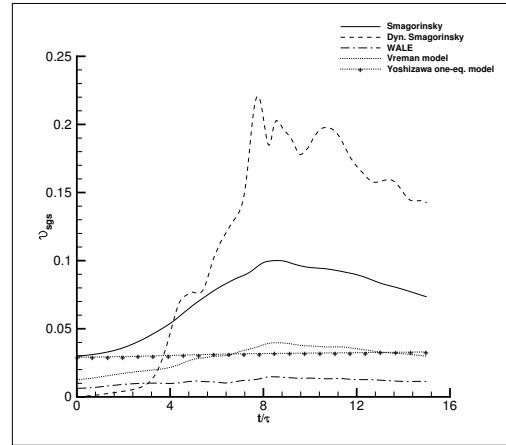
Figure 4. Evolution of enstrophy in time

Production term, $P_{k_{sgs}} = 2\nu_{sgs}\bar{S}_{ij}\bar{S}_{ij}$ in Fig.5c and 5d computed by the models on the coarse grid is wider than the fine grid solution which is narrow and accumulated around the transition time. The minimum values are given by the WALE model and the Yoshizawa one-equation model. The largest values are computed by the Smagorinsky and the Dynamic Smagorinsky models. Unlike the SGS viscosities, the production is almost independent of the grid resolution.

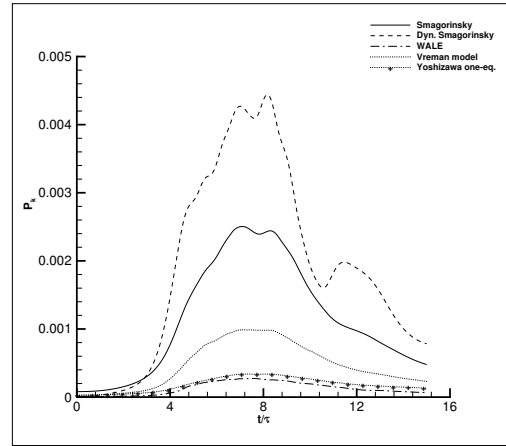
In order to observe the distribution of turbulent kinetic energy among the wave numbers, the energy spectrum is also computed at time $t/\tau = 8.2$ when the dissipation reaches its peak and plotted in Fig.6. Kolmogorov's $k^{-5/3}$ line in the inertial sub-range is also plotted for comparison. There is no noticeable difference among them in the inertial sub-range. However, at high wave numbers or smaller scales where the viscous dissipation dominates the flow (i.e., dissipation range), there is an observable difference between the Dynamic Smagorinsky and the Yoshizawa one-equation model. The Dynamic Smagorinsky model is the most dissipative in this range due to the largest contribution of μ_{sgs} to the total dynamic viscosity.



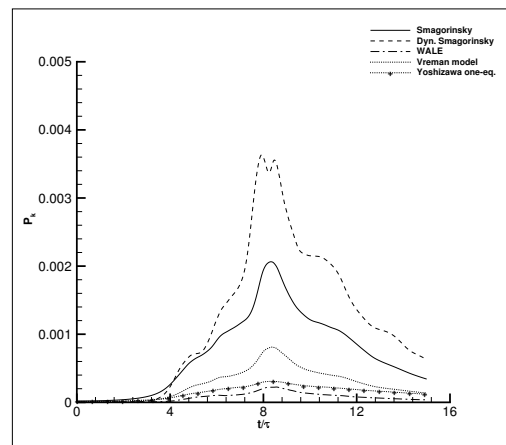
(a) Coarse grid (64^3)



(b) Fine grid (128^3)



(c) Coarse grid (64^3)



(d) Fine grid (128^3)

Figure 5. Evolution of $P_{k_{sgs}}$ term and ν_{sgs} in time

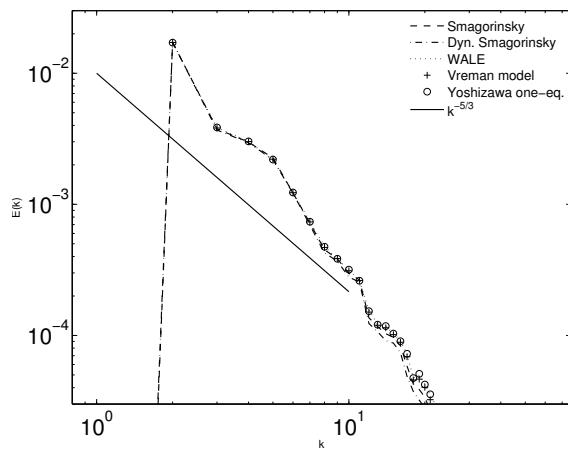


Figure 6. Turbulent kinetic energy ($E(k)$) .vs. wave number (k)

This study shows that SGS models constructed with advanced mathematical operators, which are able to describe the flow structures and their interactions in a physically correct way, produce results close to DNS by adaptively scaling their inherent dissipations. Further tests must be done for the flows including other complex features such as spatial transition and separation-reattachment regions, for better understanding of the behavior of SGS models.

ACKNOWLEDGEMENTS

IY thanks to The Scientific and Technological Research Council of Turkey (TUBITAK) for supporting his research stay in Sweden. The financial support of SNIC (Swedish National Infrastructure for Comp.) for computer time at C3SE (Chalmers Center for Comp. Sci. and Eng.) under the Project C3SE 2015/1-11 is also gratefully acknowledged.

REFERENCES

- [1] Taylor, G., and Green, A., 1937, "Mechanism of the Production of Small Eddies from Large Ones", *Roy Soc London Proc Series A*, Vol. 158, pp. 499–521.
- [2] Brachet, M., Meiron, D., Orszag, S.A. and Nickel, B., Morf, R., and Frisch, U., 1983, "Small Scale Structure of the Taylor-Green Vortex", *J Fluid Mechanics*, Vol. 130, pp. 411–452.
- [3] Davidson, L., and Peng, S. H., 2003, "Hybrid LES-RANS modelling: A One-equation SGS Model Combined with a k - ω Model for Predicting Recirculating Flows", *Int J for Num Meth in Fluids*, Vol. 43 (9), pp. 1003–1018.
- [4] Emvin, P., 1997, "The Full Multigrid Method Applied to Turbulent Flow in Ventilated Enclosures Using Structured and Unstructured Grids", Ph.D. thesis, Dept. of Thermo and Fluid Dynamics, Chalmers University of Technology.
- [5] Smagorinsky, J., 1963, "General Circulation Experiments with the Primitive Equations", *Monthly Weather Review*, Vol. 91, p. 99.
- [6] Yang, K., and Ferziger, J., 1993, "Large-Eddy Simulation of Turbulent Obstacle Flow Using a Dynamic Subgrid-Scale Model", *AIAA Journal*, Vol. 31 (8), pp. 1406–1413.
- [7] Nicoud, F., and Ducros, F., 1999, "Subgrid-Scale Stress Modelling Based on the Square of the Velocity Gradient Tensor", *Flow, Turbulence and Combustion*, Vol. 62 (3), pp. 183–200.
- [8] Vreman, A. W., 2004, "An eddy-viscosity subgrid-scale model for turbulent shear flow: Algebraic theory and applications", *Physics of Fluids (1994-present)*, Vol. 16 (10), pp. 3670–3681.
- [9] Yoshizawa, A., 1986, "Statistical theory for compressible turbulent shear flows, with the application to subgrid modeling", *Physics of Fluids (1958-1988)*, Vol. 29 (7), pp. 2152–2164.
- [10] Sreenivasan, K. R., and Antonia, R. A., 1997, "The Phenomenology of small-scale turbulence", *Annual Review of Fluid Mechanics*, Vol. 29, pp. 435–472.
- [11] Hahn, M., 2008, "Implicit Large-Eddy Simulation of Low-Speed Separated Flows Using High-Resolution Methods", Ph.D. thesis, Cranfield University, School of Engineering, Department of Aerospace Sciences.
- [12] Taylor, G., 1935, "Statistical theory of turbulence", *Proceedings of the Royal Society of London Series A, Mathematical and Physical Sciences*, Vol. 151 (873), pp. 421–444.
- [13] Pope, S., 2000, *Turbulent Flows*, Cambridge University Press.
- [14] Tennekes, H., and Lumley, J., 1972, *A First Course in Turbulence*, The MIT Press.
- [15] Landahl, T., and Mollo-Christensen, E., 1992, *Turbulence and Random Processes in Fluid Mechanics*, Cambridge University Press.
- [16] Shu, C.-W., Don, W.-S., Gottlieb, D., Schilling, O., and Jameson, L., 2005, "Numerical Convergence Study of Nearly Incompressible, Inviscid Taylor–Green Vortex Flow", *Journal of Scientific Computing*, Vol. 24, pp. 1–27.